⟨S|P|S⟩ swiss physical society

Nr. 77, November 2025

SPG Mitteilungen
Communications de la SSP

Auszug - Extrait

Physics Anecdotes and Personal Recollections (33)

Early Digital UV Plotters

Bernhard Braunecker

This article has been downloaded from:
https://www.sps.ch/articles/physics_anecdotes/

DOI: 10.5281/zenodo.18021230

Physics Anecdotes and Personal Recollections (33)

Early Digital UV Plotters

Bernhard Braunecker

Introduction

During the 1990s, significant advancements were made in the development of digitally controlled photonic systems, particularly in the field of lithography for ultraviolet (UV) and deep UV applications. Substantial investments were directed toward systems for the semiconductor industry, where nanometer-level precision was essential. Concurrently, efforts focused on developing similar UV-lithographic machines for the printing industry. These machines had less accuracy specifications, i.e. in the micrometer range, but they were designed for large-scale objects and required just as much technical expertise in optics and mechanics. A notable segment of the printing industry was the fabrication of large-format screens, covered with dense nylon meshes, often referred to as printing stencils or templates or clichés. They were and still are needed to print high resolution color patterns onto various substrates such as paper, textiles, metals, ceramics, and glass.

The manufacturing of these large templates was carried out by special lithographic machines and one needed profound engineering experience in optics, photonics, precision mechanics, control engineering, and computing. During this period in the 1990s, there was for example a high demand in the Asian society for printing historical motifs on extremely expensive silk fabrics, especially for the production of traditional Japanese kimonos. This niche market underscored the importance of advanced lithographic techniques and the integration of multidisciplinary expertise to meet the demanding quality standards and aesthetic requirements of traditional textile arts.

A printing process always begins even today with the selection of the most suitable basic colors for the image sample at hand, which can be determined using the Pantone code, for example [1]. The aim is to achieve the desired color impression with as few basic colors as possible. A stencil is required for each of these selected basic colors, which is later brought into contact with the object during the actual printing process. The color ink is usually applied by spraying on the stencil. Since the mutual position of different color pixels is tolerated to within a few µm, this requires that the stencil fabrication *per se* and the mutual alignment of different stencils is performed with the corresponding high precision.

Until the 1990s, the stencils were produced by purely optical methods. The graphic pattern for each basic color was drawn by hand, photographed and chemically developed. The transparencies were then projected onto a large-format screen using special optics with UV light. The screen consisted of a fine-meshed nylon grid of about 20 µm pitch and width coated with light-sensitive monomer photoresist. When a negative photoresist was used, the UV-exposed areas polymerized, causing them to adhere to the nylon grid, while the unexposed monomeric areas could be removed by spraying them with water, for example. This analog-optical process was time-consuming, inflexible and costly, as only trained specialists were eligible.

This changed in the 1990s with the introduction of two decisive measures, first by the computer-aided design of stencil patterns and second by the direct control of the optical projection process using digital pattern data. Both innovative steps increased process efficiency, as they enabled significantly shorter throughput times, led to more production stability, and they can be largely automated to reduce costs.

R & D Project

Leica Geosystems together with the Danish company Mografo, a subsidiary of the LEGO Group at the time, developed the DISE concept (Direct Screen Exposure) at the end of the 1990s and built the first prototypes and a pilot series of 20 machines (Fig. 1). As the photoresists of the time were still rather insensitive to light in the UV range, a spot-to-spot exposure concept was chosen with a large and expensive Ar-ion laser as light source in order to keep exposure times short. Large screen sizes of 1.85 m × 7 m were specified, and standard screens of size 1.85 m × 1.5 m had to be exposed in about 10 minutes with pixels of 20 µm spot diameter. This led to the construction of a highly complex mechanical *Step and Repeat* machine, the same concept as applied in the semiconductor lithography.

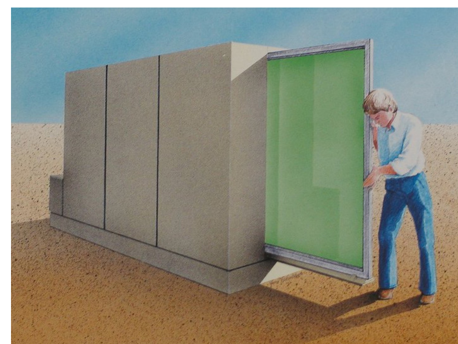

Fig. 1: DISE 3, loading the printing screen

Technical Layout

The conceptual design of the DISE system is shown in Fig. 2, with the blue line representing the UV laser beam. The laser was a large and water-cooled 4 W argon ion laser from Spectra Physics, which emitted around 1 W in the UV range at 365 nm. The amplitude of the laser beam was modulated by an EO-modulator fed with the binary image pixel data stream at a maximum frequency of 10 MHz. To correct thermally induced instabilities of the beam axis in the laser tube, a galilean beam expander (BEX) with two lenses followed next. Its primary lens could be moved by motor in both directions perpendicular to the beam axis to readjust the beam direction in real time, while its secondary lens mounted on a piezo driver allowed to correct any defocus of the beam

1 The colors in screen printing are determined using Pantone codes (solid coated) and then precisely mixed to achieve the desired color quality https://www.cantana.com/service/siebdruck/

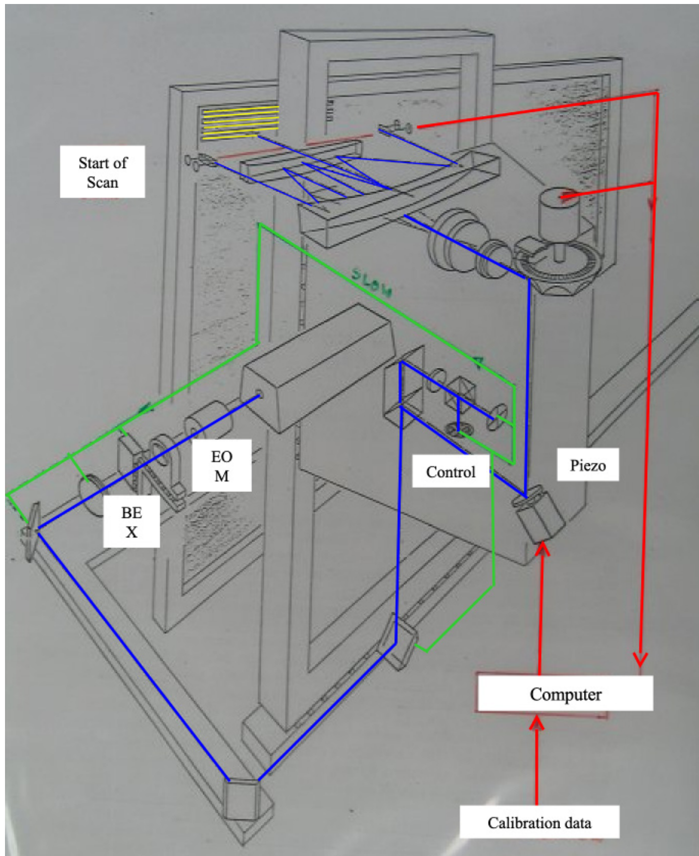

Fig 2: DISE 3: The laser beam (blue lines) exposes the screen (yellow lines). The writing process is controlled by a slow closed control loop (green lines) and a fast open control loop (red lines).

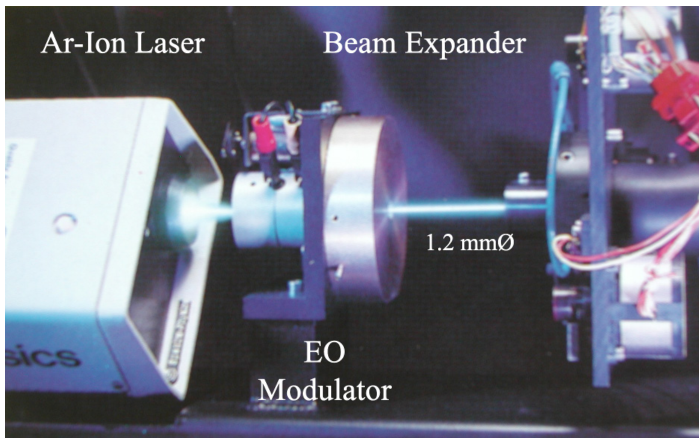

Fig. 3: Laser, EO Modulator and BEX

(Fig. 3). The laser beam was then guided into a meter-long mirror carrier module in which two mirrors could be moved by motor to correct any lateral offset error of the beam axis.

The beam was then directed to the scanner head, which was precisely movable by motor in the vertical y and the horizontal x-direction. A special control module was installed at the entry aperture to monitor in real-time both alignment errors. To this purpose a beam splitter divided the laser beam into two parts, where the one with about 2 % of the total intensity was focused with an auxiliary lens onto two four-quadrant detectors, one of which was installed 5 mm before and the other 5 mm after the nominal focus. Calculating the sum and difference of both measured center of gravity coordinates and also the size of the spot diameter allowed to determine the 2D-offset and the 2D-direction errors of the beam axis and also the defocus, and, consequently, drive both BEX lenses and the two deflection mirrors in a closed control loop which is shown as green lines in Fig. 2.

Scanning Concept

The other part of the laser beam with 98 % of the total intensity was reflected by the beam splitter and directed to a fast steerable piezo mirror and from there to a fast rotating polygon wheel with seven mirror facets (Fig. 4). While the piezo mirror could only tilt the beam by a few angular degrees in ± y-direction, the beam was deflected by each of the facets between ± 25.7° in the horizontal x-direction, called the swath direction. Since only parts of the mirror surface were used (η_{Fill} = 0.8), the effective deflecting angle was ± 20.6°. The deflected beam was then focused onto the raster screen by a special optical unit consisting of a F-theta collimator (Box 1) and a strip-shaped, off-axis catadioptric mirror

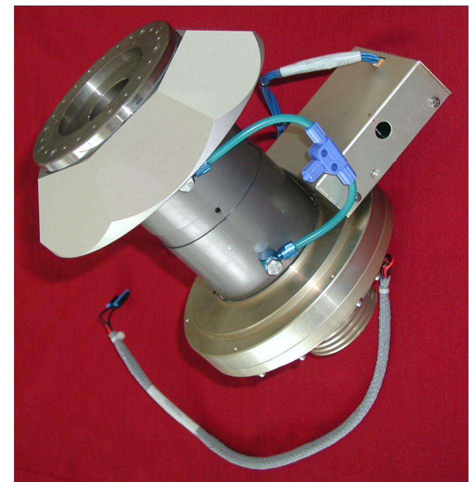

Fig. 4: Polygon wheel with 7 Facets

Box 1: F-theta Optics

Normally, an optic is corrected according to $x = F \cdot \tan(\theta)$ with θ the field angle. With scanner optics, however, the distortion is adapted that the beam deflection occurs according to $x = F \cdot \arg(\theta)$. The advantage is that with a constant angular velocity ω of the scanner mirror, this results in a constant spot velocity $v = dx / dt = F \cdot d\theta / dt = F \cdot \omega$ along the writing line. The pulse laser can then be operated with a constant shooting frequency $f_{pulse} = 1/\Delta t_{pulse}$ in order to obtain an aquidistant spot distribution $\Delta x = v \cdot \Delta t_{pulse} = F \cdot \omega \cdot \Delta t_{pulse}$.

Raster Screen	Optics	Polygon Wheel	
1.85 m × (1.5 m to 7 m) ⇒ A_{Raster} = 2.78 m² to 12.95 m²	Photoresist: Sensitivity S_{Resist} = 5 mJ / cm² at 365 nm	$\Omega_{Polygon}$ = 60 Hz ⇒ $T_{Polygon}$ = 16.6 ms	No of facets: N_{Facet} = 7 ⇒ T_{Facet} = 2.4 ms
Nylon mesh density ≈ 20 μm			
Swath length L_{Swath} = 380 mm (15 ″)	⇒ $F_{Optik} = L_{Swath} / \Theta_{Beam}$ = 530 mm	Facet fillfactor: η_{Fill} =0.8 ⇒ $T_{Effective}$ = 1.9 ms	⇒ Beam deflection Θ_{Beam} = ± 180°/ $N_{Facet} \cdot \eta_{Fill}$ = ± 20.6°
⇒ $v_{Swath} = L_{Swath}/T_{Effective}$ = 200 m/s			

Table 1: System Data

system. Both parabolic mirrors were decentered and tilted that the beam hit the screen with a normal incidence angle (Fig. 5). In order to write a swath line of length L_{Swath} = 15″ = 380 mm by each facet, the total focal length of the optical scanning unit had to be F = 530 mm (Table 1).

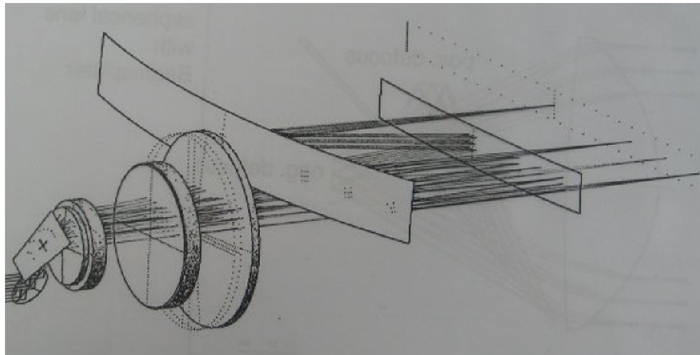

Fig. 5: Optical system with F-theta lens collimator and two-mirror telescope. Left a facet mirror and below the piezo mirror.

Operating Mode

The scanner head was moved in y-direction from top to bottom at the constant speed $v_{Scanhead} = \delta y_{Pix}/T_{Facet}$, where δy_{Pix} is the pixel diameter and T_{Facet} the time of a full facet deflection, to assure a seamless continuation in y of adjacent x-writing lines. The seamless pixel position in x-direction was achieved by the F-theta design of the optics, allowing a constant shooting frequency of the EO-Modulator. In order to precisely level the x-writing lines on the screen, the laser beam had to be moved slightly in y-direction during the x-scan. The values of this y-correction were part of the reference data for the piezo mirror. They are characterized by the angle $w_{Back} = \eta_{Fill} \cdot \delta y_{Pix}/L_{Swath}$, which depends similar as $v_{Scanhead}$ on the choice of the pixel size (Table 1).

All these manipulations resulted in a perfectly aligned and homogenously distributed spot pattern at the screen, i.e. without any gap between adjacent pixels. In order to maintain the perfect pattern geometry in the case of a small displacement of the screen of ± 2 mm along the beam direction, called depth-of-focus DoF, the mirror telescope was designed as telecentric, i.e. with normal incident angle tolerated to ± 10 mrad, to keep the pixel position within ± 20 μm. When the scanner head reached the lower y-setting limit of the scanning screen, it was moved by 380 mm in x direction and driven back to the upper setting value. However, the connection error between adjacent frames had to be maintained within ± 10 μm, another very challenging demand.

Table 2 shows the values of some scanning parameters as function of the pixel spot diameter at the raster screen, which could be set by the operator between 20 μm and 40 μm, corresponding to a write density of 1270 dpi to 635 dpi.

Fast Control on Track

The specified positional accuracy of ± 5 μm of a pixel at the raster screen corresponded to a beam deflection error of ± 10 μrad or approximately ± 2 arcsec concerning the focal length F = 530 mm. As the pyramidal angle of the facets could already scatter by ± 10 arcsec due to manufacturing limitations, which was equivalent to a pixel offset of ± 56 μm in y-direction, this so-called *line curvature error* had to be corrected *on track* individually for each facet by the piezo mirror. The fast correction was run in an open loop mode using reference data, which were obtained by a calibration process. Thereby a 380 mm long film strip was exposed by a selection of about 30 pixels from each of all seven facets.

During the test phase, it became apparent that the DoF range, i.e. the installation position of the screen, was too narrow specified at ± 2 mm and had to be extended to about ± 5 mm. In order to maintain the critical telecentricity, the axis of rotation of the polygon had to be tilt-

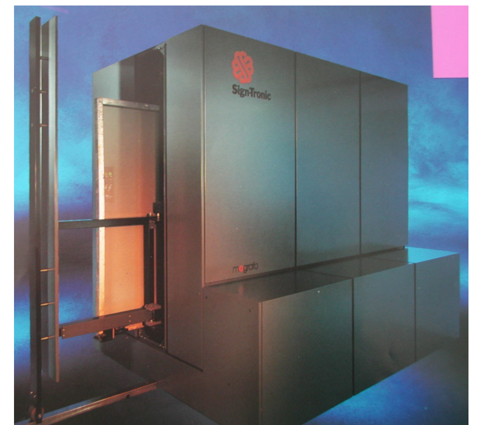

Fig. 6: Computer to Screen Machine from Signtronic (about 2005).

Box 2: F-theta Correction on the Track

It turned out that the axis of rotation of the polygon wheel had to be tilted forward by a few angular degrees due to the off-axis mode of the reflector telescope. This tilt improved the imaging quality, assured telecentricity for a larger DoF and reduced the line curvature error. However, this led to a small rotation angle-dependent F-theta error, which had to be corrected by slightly varying the pulse frequency. The F-theta correction data for each facet were determined during calibration and stored for fast control during operation.

Write Density (dpi)	Spot Diameter $\delta x_{Pix} = \delta y_{Pix}$ (μm)	EO-Frequency f_{Pulse} (MHz)	$v_{Scanhead}$ (mm/s)	w_{Back} (μrad)	Write Rate W_{Rate} (cm²/s)	Laser Power P_{Laser} (W)	Total Exposure Time T_{Total} (min) for 1.85 × 1.5 m screen
1270	20	10	8.4	42	40	0.2	11.6
847	30	6.7	12.6	63	60	0.3	7.7
635	40	5.0	16.8	84	80	0.4	5.8

Table 2: Operating Data

Definitions:
$f_{Pulse} = v_{Swath} / \delta x_{Pix}$ $v_{Scanhead} = \delta y_{Pix} / T_{Facet}$ $w_{Back} = \eta_{Fill} \cdot \delta y_{Pix} / L_{Swath}$
$W_{Rate} = \delta y_{Pix} \cdot v_{Swath}$ $P_{Laser} = S_{Resist} \cdot W_{Rate}$ $T_{Frame} = A_{Raster} \cdot W_{Rate}$

ed minimally around the x-axis. The disadvantage was that any y-correction by the piezo mirror also produced a small amount of F-theta error, which must be compensated and had to be part of the reference data (Box 2). When later in operation the laser beam passed a start-of-scan sensor the digitally stored y-reference data steered the piezo mirror to compensate line curvature and to horizontally level the swath line, while the x-reference data were used to slightly adapt the pulse frequency of the EO-Modulator to correct the position error in x-direction.

Alternative Concepts

The described spot-to-spot method was characterized by its high writing speed v_{Swath} = 200 m/s and position accuracy of ± 5 μm, but also by its high complexity and substantial costs, primarily due to the reliance on expensive components such as ion-lasers, electro-optic modulators, and polygon wheels, and prompted the printing industry to seek alternative solutions. With the advent of new technologies in the early 2000s, including powerful UV-LED sources, more sensitive photoresist materials, and Micro-Electro-Mechanical Systems (MEMS)-based devices, innovative printing approaches emerged. The most promising solution utilized a digital light projector DLP, i.e. a MEMS micromirror array, where each micromirror element, which is mechanically supported by several micro-flexures, could be tilted by several degrees when applying an electrical signal. The main advantage was that projecting the chip-array on the screen transferred the precise pixel arrangement of the lithographic MEMS manufacturing process. The idea is that only reflected light from uninclined mirror pixels could expose the photoresist, while light from an actively tilted mirror was optically blocked, or vice-versa (Fig. 7) [2].

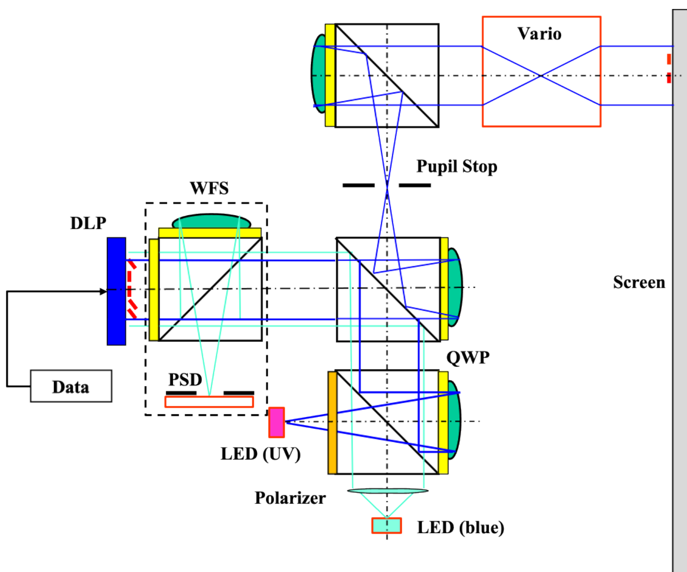

Fig. 7: Optical Head (Study of Leica from 2005), where a plane wavefront of UV illuminates a DLP (blue lines for pupil rays). Reflected light from uninclined DLP micromirrors is imaged onto the screen, otherwise blocked by the pupil stop. The cyan lines illustrate how to measure the flatness of the wavefront reflected from the DLP if all elements are not tilted, using a special wavefront sensor WFS. Parabolic imaging mirrors are marked in green, polarizers in orange and quarter-wave plates QWP in yellow. They lead to s-polarized reflected and p-polarized transmitted UV light in the four beamsplitter cubes. The afocal vario objective can be tuned for the desired spot size at the screen.

To expose meter-sized screens the optical head including DLP and projection optics had to be mechanically stepped in x and y-direction, always keeping the connection error within the specifications. Proved methods to control the 2D-motion of a small optical unit across large areas were developed at that time, mainly for big space projects at ESA, and were considered as possibility to control and correct the frame-to-frame connection [3].

The other critical question was how reproducible were the zero tilt angles of the mirror elements after once deflected? Does the residual angular jitter allow to reach the specified pixel position accuracy of ± 5 μm at the screen? The measurement idea was to deflect all pixels as a collective, return to deflection angle zero and measure the reflected and perhaps distorted plane wavefront with a Shack-Hartmann WFS sensor, which was easily to integrate in the optical layout. Since this would only work for systems with a short focal length F of typical 25 mm, Leica proposed a more sensitive method, originally developed for ESA for intersatellite data communication with lasers, which should be applicable for the case of larger F values with the DLP in *dual-use*. Fig. 7 shows the concept, where besides the projection with UV light onto the screen (blue lines), the DLP was also illuminated by a plane wave of visible blue light. The reflected DLP wavefront was fouriertransformed, i.e. focused on a Position Sensitive Detector PSD (cyan lines). The DLP was then switched to a series of orthogonal 2D patterns of macropixels, consisting of a block of micromirror elements, and their average phase distortion could be retrieved from all measured PSD signals with high resolution [4]. The phase information, i.e. the local angular deviation, could be used e.g. to precorrect the image data.

Despite the impressive print systems, Leica decided at the time to focus on its core competence of measurement technology and not on writing systems, so that the activities after DISE could not be further continued. Today the DLP technology is well established in the printing industry, and a good overview of the current state of the art is given in a booklet of the Swiss company *Signtronic* [5].

2 Texas Instruments, the pioneer of the DLP technology, offers arrays with e.g. 1920 × 1080 mirrors with 10.8 μm pitch and ± 12° tilt angle (relative to flat state), leading to an active DLP diameter of 0.95-inch diagonal. DLP9500UV DLP® 0.95-Inch UV 1080p 2x LVDS Type A Digital Micromirror Device https://www.ti.com/

3 "Testing large optical Systems", *SPG Mitteilungen* Nr. 73, p. 49 (2024). Here we showed how to get rid of unavoidable motion errors when scanning large optical areas with small optical modules. https://sps.ch/de/articles/physics_anecdotes

4 "Optical Wavefront Sensing", *SPG Mitteilungen* Nr. 72, p. 38 (2024). Here we described the idea of using a Digital Light Projector as wavefront sensor. https://sps.ch/de/articles/physics_anecdotes

5 https://signtronic.com/en/